Supporting Information

Modulation of oxygen vacancies influences electrocatalytic performance of Ni-doped Ceria for oxygen and hydrogen evolution

Ajit Kumar Dhanka[a], Mayank Tiwari[b], Prashant K. Bhartiya[b,c], Balaram Pani[d], Avneesh Mittal[e], Debabrata Mishra*[b], and Nityananda Agasti*[a]

[a] Department of Chemistry, University of Delhi, North Campus, Delhi 110007, India

[b] Department of Physics and Astrophysics, University of Delhi, North Campus, Delhi 110007, India

[c] Delhi School of Climate Change and Sustainability, Institution of Eminence, University of Delhi, 110007

[d] Department of Chemistry, Bhashkaracharya College of Applied Sciences, University of Delhi, Dwarka, New Delhi, 110075, India.

[e] Department of Electronics, Bhaskaracharya College of Applied Sciences, University of Delhi, Dwarka, New Delhi, 110075, India.

SUPPORTING INFORMATION CONTENT

TABLE OF CONTENTS

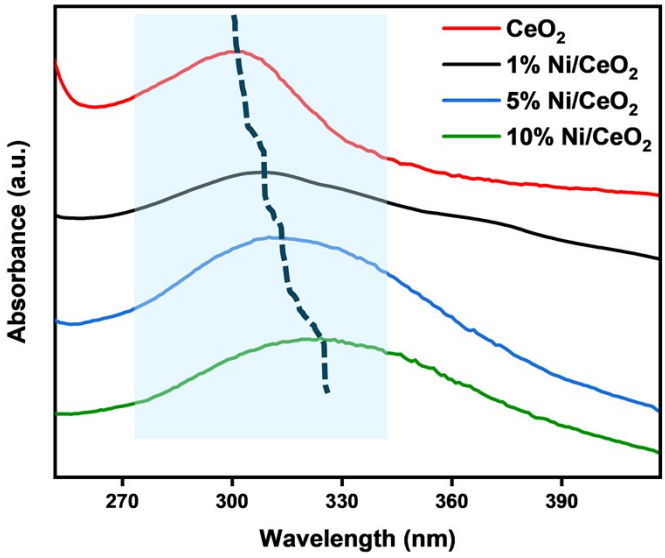

Fig. S1 The shifting of UV-vis. absorption band of CeO_2 on Ni-doping.

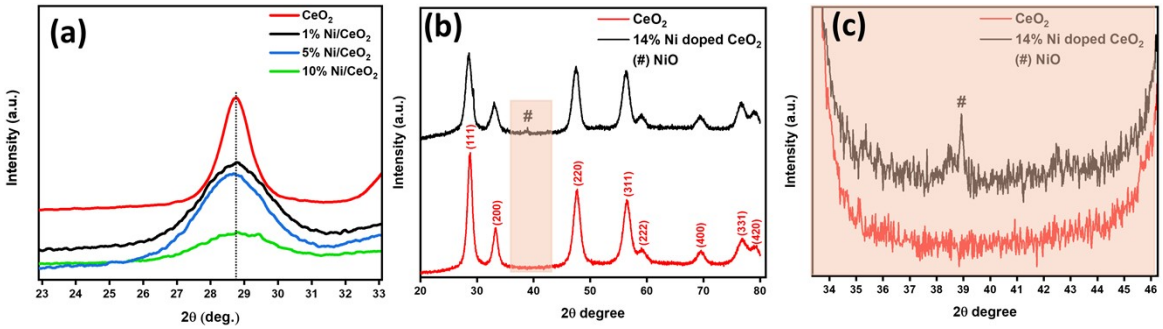

Fig. S2 (a) Variation in intensity of peaks in XRD for CeO_2 and Ni-doped CeO_2 [1], (b) XRD pattern of Ni-doped CeO_2 with 14% Ni, and (c) zoom pattern of the peak corresponding to NiO appearing in Ni-doped CeO_2 with 14% Ni.

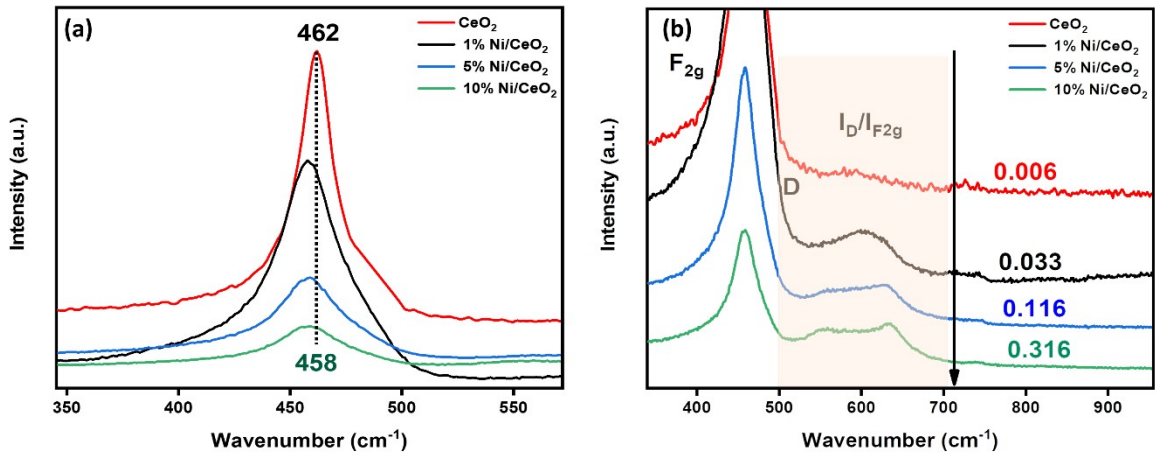

Fig. S3 (a) Variation in intensity, broadening, and shifting of Raman peaks and (b) the bands at 610 cm^{-1} correspond to the defect-induced mode (D) for CeO_2 and Ni-doped CeO_2 [2,3].

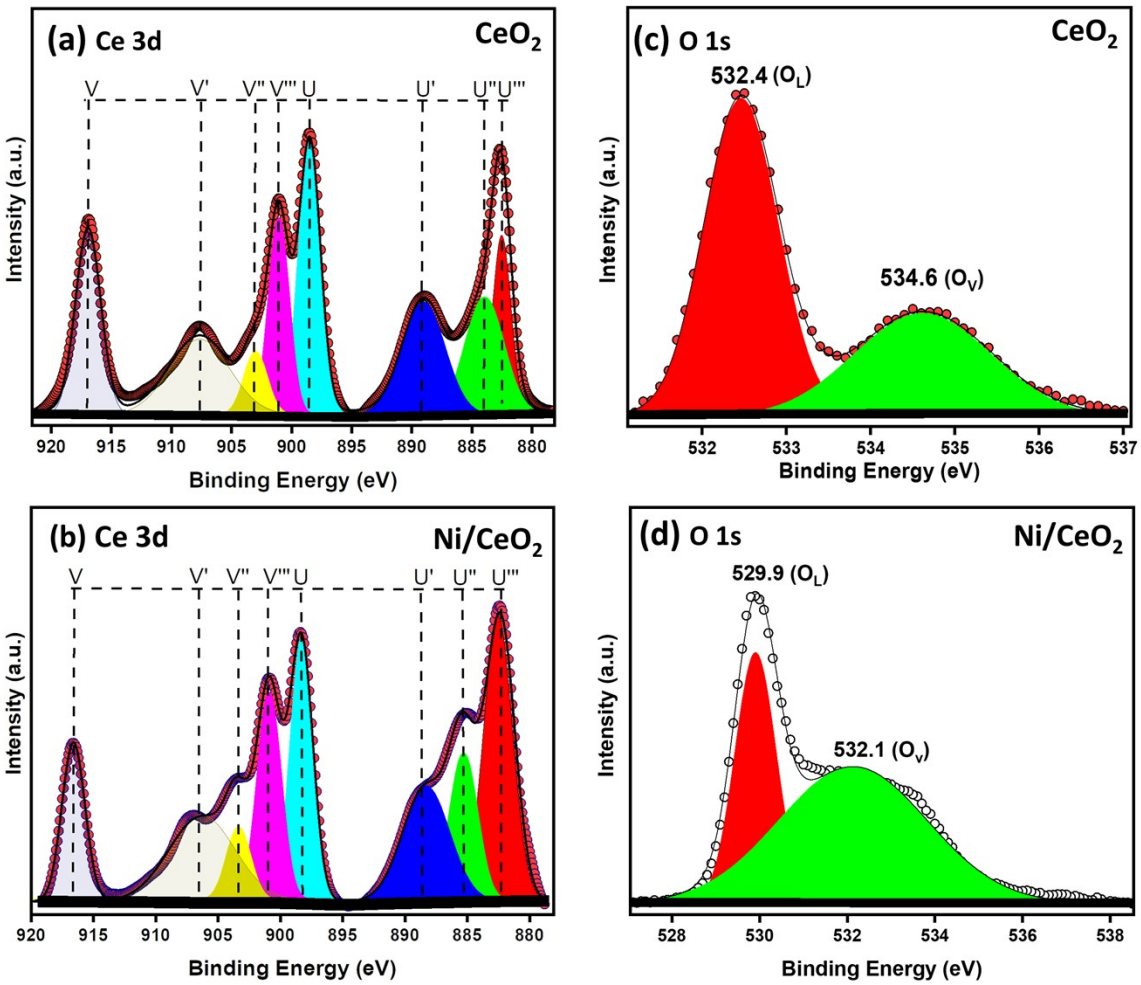

Fig. S4 (a) and (b) the relative integral area Ce 3d, (c) and (d) the integral area of O 1s for CeO_2 and Ni/CeO_2.

The relative concentration of Ce^{3+} was determined by calculating the ratio of the Ce^{3+} peak area to the total area under the Ce 3d spectrum. For the 10% Ni/CeO_2 sample, the Ce^{3+} content was found to be approximately 25.17%, which is notably higher than the 14.39% observed for pure CeO_2. This increase in Ce^{3+} concentration upon Ni incorporation suggests an enhancement in oxygen vacancy formation, likely due to the strong interaction between Ni and CeO_2[4].

The relative percentage of Ce^{3+}, determined by integrating the area under the corresponding peaks for undoped CeO_2 and Ni/CeO_2. The ratio of the area of peaks corresponding to Ce^{3+}

to the area of the peaks corresponding to all peaks was used as an indicator of the concentration of oxygen vacancies associated with Ce^{3+} sites on the catalyst surface[5].

Table S1: The relative amounts (%) of Ce^{3+} were calculated from the areas under the curves.

Label	**Binding energy (eV)**	**CeO_2 (Area)**	**Binding energy (eV)**	**Ni/CeO_2 (Area)**
U‴	882.5	10102.9	882.3	14440.5
U″	883.9	13691.2	885.2	7064.6
U′	889	14450.4	888.3	9387.9
U	898.5	17959.2	898.3	10627.3
V‴	901	12020.3	900.8	8463.6
V″	902.9	4370.7	903.3	3017.5
V′	907.6	13885.6	906.3	9891.2
V	916.9	14082.3	916.6	6452.5
	Ce^{3+}	(10102.9+4370.7) **= 14473.6**	**Ce^{3+}**	(14440.5+3017.5) **= 17458**
	Total Area of Ce 3d	**100562.6**		69345.1
	% of Ce^{3+} = Area of Ce^{3+}/ Total Area	**14473.6 / 100562.6**		17458/69345.1 **=25.17 %**

		=14.39%		

Table S2: The relative integral area of the O 1s peak calculated from the spectra[6].

CeO_2			**Ni/CeO_2**	
Peaks assignment	**Binding Energy (eV)**	**Area (A)**	**Binding Energy (eV)**	**Area (A)**
O_L	532.4	7907.02	529.9	9335.4
O_V	534.6	4783.60	532.1	18301.5
O_V/O_L		**0.6**		**1.9**

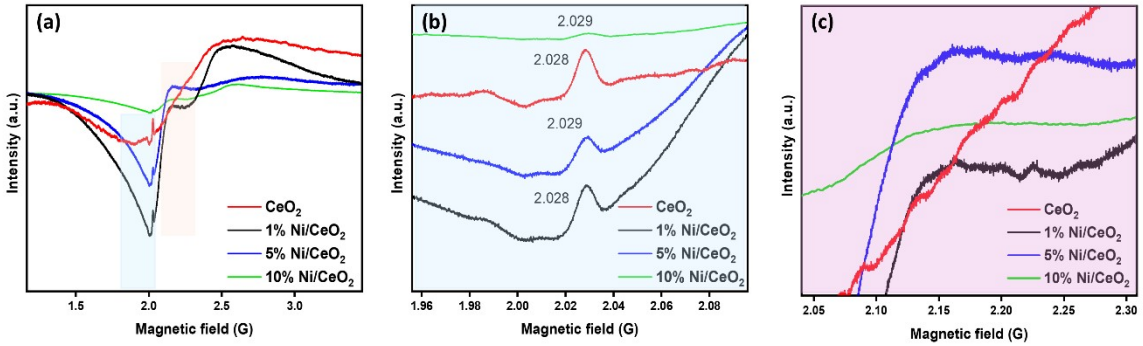

Fig. S5 (a) EPR spectra of pristine and doped CeO_2, (b) Zoomed EPR signals, from the region highlighted in blue, with their respective g-values, and (c) Zoomed EPR signals, from the region highlighted in pink (in the range of g = 2.07 to 2.15) showing additional bands in Ni-doped CeO_2[7].

The intensity of the EPR spectra decreases as the concentration of Ni increases, as shown in the enlarged EPR spectra (**Fig. S5 b).** The lowest intensity of the EPR spectra for

Ni/CeO_2 with 10% Ni suggests maximum oxygen vacancy defects. Further, there is an additional band with G in the range of 2.07 to 2.15 observed in Ni/CeO_2, and the same is absent in pristine CeO_2. This suggests the presence of Ni-related paramagnetic centres and modified defect states in doped ceria.

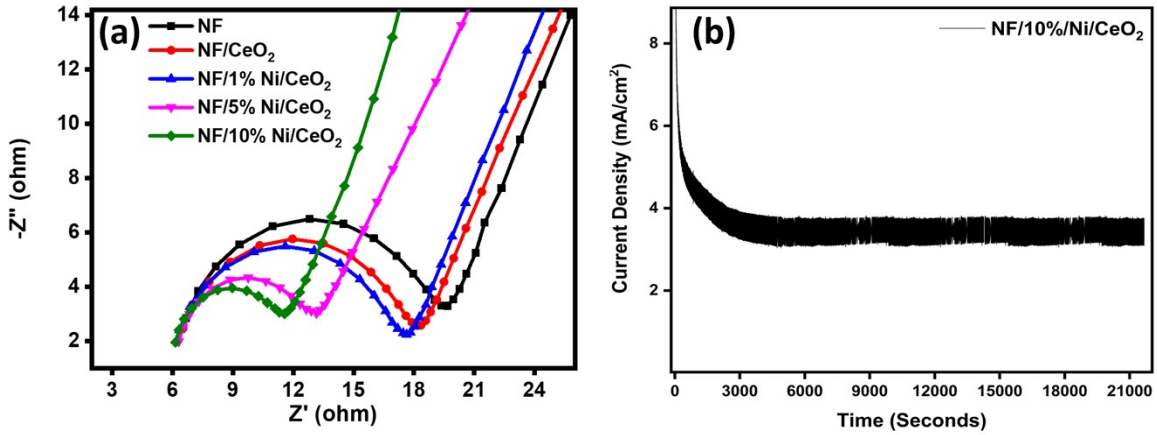

Fig. S6 (a) Nyquist Plot (EIS) for NF/CeO_2 and NF/1,5,10% Ni/CeO_2 electrodes, measured in 1 M KOH with a 10-mV amplitude over a frequency range of 10^5–10^0 Hz and (b) Chronoamperometric curve at a constant potential of 1.48 V (vs RHE) for the NF/10% Ni/CeO_2 electrodes.

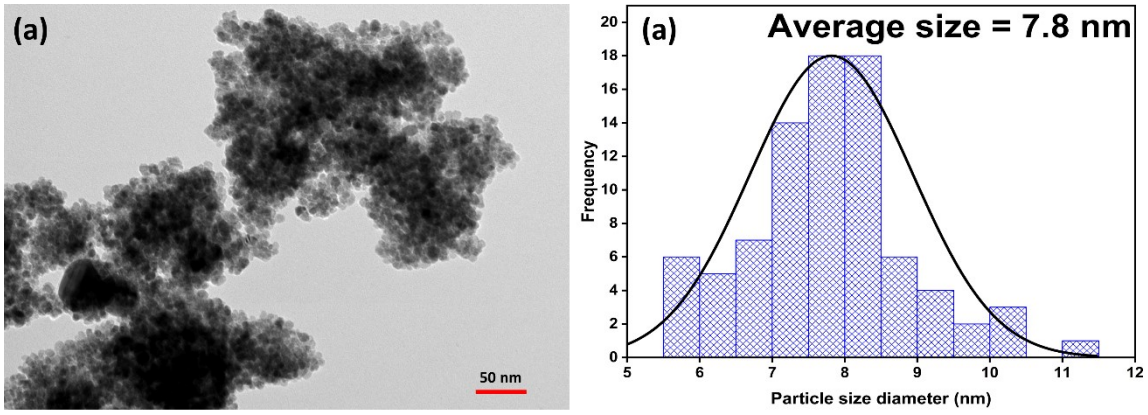

Fig. S7 (a) Low-resolution TEM image of CeO_2, and (b) the average particle size calculated from the TEM image of Ni/CeO_2.

References

1. Dhanka, A. K., Kohlrausch, E. C., Samantray, R., Kumar, V., Pani, B., & Agasti, N. (2025). Harnessing defects in Ag/CeO_2 for enhanced photocatalytic degradation of antibiotic in water: Structural characteristics, in-depth insights on mechanism, degradation pathway. *Chemical Engineering Journal Advances*, *21*, 100706. https://doi.org/10.1016/j.ceja.2025.100706

2. Jayakumar, G., Irudayaraj, A. A., Raj, A. D., Sundaram, S. J., & Kaviyarasu, K. (2022). Electrical and magnetic properties of nanostructured Ni doped CeO_2 for optoelectronic applications. *Journal of Physics and Chemistry of Solids*, *160*, 110369. https://doi.org/10.1016/j.jpcs.2021.110369

3. Jafari, S., & Shaghaghi, Z. (2023). CeO_2/CuO/NiO hybrid nanostructures loaded on N-doped reduced graphene oxide nanosheets as an efficient electrocatalyst for water oxidation and non-enzymatic glucose detection. *Dalton Transactions*, *52*(22), 7564-7580. https://doi.org/10.1039/D3DT00527E

4. Dhanka, A. K., Pani, B., & Agasti, N. (2025). Defect-enriched CuO/CeO_2 nanostructure: in-depth structural characterization and photocatalytic performance. *RSC advances*, *15*(15), 11774-11789. https://doi.org/10.1039/D5RA00640F

5. Soni, S., Vats, V. S., Kumar, S., Dalela, B., Mishra, M., Meena, R. S., & Dalela, S. (2018). Structural, optical and magnetic properties of Fe-doped CeO_2 samples probed using X-ray photoelectron spectroscopy. *Journal of Materials Science: Materials in Electronics*, *29*(12), 10141-10153. https://doi.org/10.1007/s10854-018-9060-x

6. Dhanka, A. K., Tiwari, M., Bhartiya, P. K., Pani, B., Agasti, N., & Mishra, D. (2025). Oxygen vacancies induced low overpotentials of Ag/CeO_2 for electrocatalytic evolution of oxygen and hydrogen. *Materials Advances*, *6*(11), 3716-3729. https://doi.org/10.1039/D5MA00321K

7. Wang, L., Yu, Y., He, H., Zhang, Y., Qin, X., & Wang, B. (2017). Oxygen vacancy clusters essential for the catalytic activity of CeO_2 nanocubes for o-xylene oxidation. *Scientific reports*, *7*(1), 1-11. https://doi.org/10.1038/s41598-017-13178-6